Pergamon

*Int. J. Heat Mass Transfer.* Vol. 41, No. 10, pp. 1199–1204, 1998

Printed in Great Britain
0017–9310/98 $19.00+0.00

PII: S0017–9310(97)00210–X

# The storage capacity of a harmonically heated slab revisited

EUGEN MAGYARI and BRUNO KELLER

Chair for the Physics of Buildings, Institute of Building Technology, Swiss Federal Institute of Technology (ETH) Zurich, CH-8093 Zurich, Switzerland

(*Received* 13 *March* 1997 *and in final form* 17 *July* 1997)

**Abstract**—The physical origin of the well-known maximum occurring in the dynamic heat storage capacity of a harmonically excited slab is analysed in terms of the fundamental solutions of Fourier's equation. It is shown that, in addition to this maximum, an infinite sequence of exponentially decaying lateral minima and maxima occur which are generated by a coherent superposition of two thermal waves propagating in opposite directions within the slab. By passing from the parabolic to the hyperbolic description of heat conduction, this effect becomes much more pronounced. © 1998 Elsevier Science Ltd.

## 1. INTRODUCTION

The storage capacity of a harmonically heated slab has attracted recent interest in connection with the contemporary energy-saving efforts in general and the passive-solar buildings in special [1]. In this respect one encounters in the technical literature experimental [1] and theoretical [2] results which find for the heat-storage capacity of a slab (excited harmonically at one and insulated adiabatically at the other boundary) as a function of its thickness, a curve which first rises towards a maximum nearly linearly, and then descends to an asymptotic value (the storage-capacity of a semi-infinite medium) smoothly.

Our aim in the present note is to show that (a) the maximum of the storage-capacity is not a solitary one as believed commonly, but it is accompanied (with increasing thickness of the slab) by a sequence of exponentially decaying lateral minima and maxima (Figs 1 and 2), (b) the maxima and minima arise as a consequence of a coherent superposition of two basic thermal waves (the fundamental solutions of the Fourier equation) propagating in opposite directions within the slab (Fig. 3), and (c) if one passes from the parabolic (Fourier) heat conduction equation to a hyperbolic (Vernotte–Cattaneo) one, the effect becomes much more pronounced (Fig. 4).

## 2. BASIC EQUATIONS AND SOLUTIONS

The starting point of our considerations is the energy conservation equation and Fourier's law:

$$\rho c\frac{\partial T}{\partial t}(x,t)+\frac{\partial q}{\partial x}(x,t)=0$$

$$q(x,t)=-\lambda\frac{\partial T}{\partial x}(x,t)\quad 0<x<d,\ t\geqslant 0 \qquad (1)$$

The left boundary ($x=0$) of the slab is heated harmonically, whereas its right boundary ($x=d$) is kept insulated adiabatically:

$$T(0,t)=T_0\cos\omega t,\quad q(d,t)=0,\quad t\geqslant 0 \qquad (2)$$

Because we are interested in the harmonic response in the slab (which governs the system after the transients have died out), we pass from real to complex quantities according to the usual prescriptions:

$$T(x,t)\to\hat{T}(x,t)=\hat{T}(x)\exp(i\omega t)$$
$$q(x,t)\to\hat{q}(x,t)=\hat{q}(x)\exp(i\omega t) \qquad (3)$$

where, in accordance with the boundary conditions (2):

$$\hat{T}(0)=T_0\quad\text{and}\quad\hat{q}(d)=0 \qquad (4)$$

In this way, the physical quantities will be recovered from the final equations by taking the real part of the corresponding complex ones.

By assuming constant thermophysical properties, the system (1) can be solved in the present case easily. Its complex solution, satisfying the boundary conditions (2), reads as:

$$\hat{T}(x,t)=T_0\left[A_+\,\mathrm{e}^{+\frac{x}{\sigma}}\mathrm{e}^{i\left(\omega t+\frac{x}{\sigma}\right)}+\mathrm{A}_-\,\mathrm{e}^{-\frac{x}{\sigma}}\mathrm{e}^{i\left(\omega t-\frac{x}{\sigma}\right)}\right]\equiv[\hat{T}_+(x)+\hat{T}_-(x)]\,\mathrm{e}^{i\omega x}$$

$$\hat{q}(x,t)=-(1+i)\frac{\lambda}{\sigma}T_0\left[A_+\,\mathrm{e}^{+\frac{x}{\sigma}}\mathrm{e}^{i\left(\omega t+\frac{x}{\sigma}\right)}-\mathrm{A}_-\,\mathrm{e}^{-\frac{x}{\sigma}}\mathrm{e}^{i\left(\omega t-\frac{x}{\sigma}\right)}\right]\equiv[\hat{q}_+(x)+\hat{q}_-(x)]\,\mathrm{e}^{i\omega t} \qquad (5)$$

where

**NOMENCLATURE**

| | |
|---|---|
| $A_{\pm}$ | amplitudes, eqn (6) |
| $a$ | thermal diffusivity, eqn (6) |
| $c$ | specific heat |
| $d$ | slab-thickness |
| $i$ | $\sqrt{-1}$ |
| $n$ | natural number |
| $Q$ | heat-storage capacity |
| $q$ | heat flux |
| $T$ | temperature |
| $t$ | time |
| $v$ | phase-velocity, eqn (7) |
| $x$ | position coordinate |
| $z$ | dynamic thickness, eqn (6). |

Greek symbols

| | |
|---|---|
| $\gamma$ | parameter, eqn (23) |
| $\Lambda$ | wavelength, eqn (7) |
| $\lambda$ | thermal conductivity |
| $\rho$ | density |
| $\sigma$ | penetration length, eqn (6) |
| $\tau$ | dimensionless time, $\tau = \omega t$ |
| $\omega$ | excitation frequency. |

Subscripts

| | |
|---|---|
| $\pm$ | fundamental solutions |
| $\infty$ | semi-infinite medium |
| $H$ | hyperbolic. |

Superscripts

| | |
|---|---|
| $\hat{}$ | complex quantity ($T$ and $q$) |
| $\tilde{}$ | support function, eqn (18) |
| $\bar{}$ | $Q$ as function of $z$ only |
| * | starting moment of the half-period. |

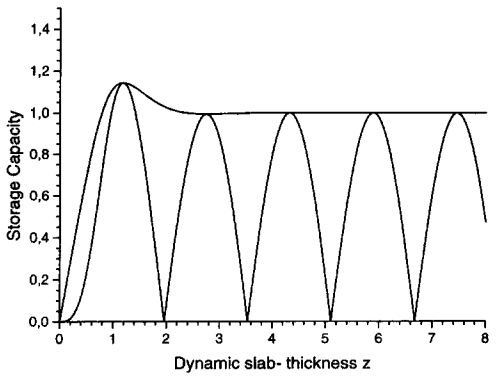


Fig. 1. The storage-capacity curve and below it the "support-curve" as given by eqns (11) and (18), respectively. The support-curve points just to the subsequent maxima and minima of the capacity-curve.

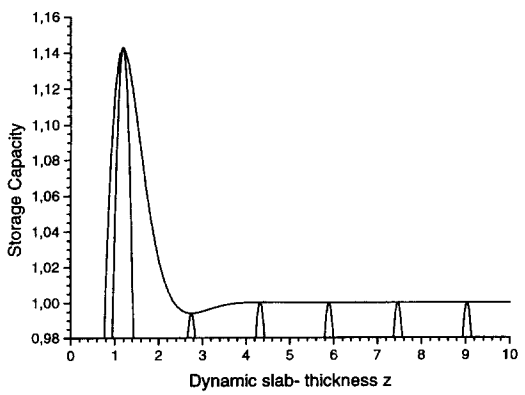


Fig. 2. Detail of Fig. 1 in which, due to the numerical magnification, also the first minimum of the storage capacity becomes visible.

$$A_{\pm} = \frac{1}{2}[1 \mp \tanh(1+i)z], \quad z = \frac{d}{\sigma},$$

$$\sigma = \sqrt{\frac{2a}{\omega}} \quad \text{and} \quad a = \frac{\lambda}{\rho c} \tag{6}$$

$\sigma$ denotes here the "penetration length" of thermal waves in the material considered, $a$ is its thermal diffusivity and $z$ denotes the "dynamical thickness" of the slab.

A simple inspection of eqns (5) leads to the following physical picture. The complex temperature and flux fields are superpositions of plane waves propagating in the slab with decreasing amplitudes from right to left (+) and from left to right (−), respectively, with the same phase-velocity v and having the same wavelength $\Lambda$:

$$v = \sigma\omega = \sqrt{2a\omega} \quad \Lambda = 2\pi\sigma \tag{7}$$

The wavelength $\Lambda$ decreases as $\omega^{-1/2}$ with increasing excitation-frequency $\omega$, but it is independent of the boundary condition at $x = d$ and the thickness $d$ of the slab. In addition to the excitation-frequency $\omega$, it only depends on the thermal diffusivity of the material considered. According to eqn (7) the wavelength $\Lambda$ of these dispersive waves is aproximately six times larger than the penetration length $\sigma$. This special circumstance leads to a quite paradoxical of behaviour of thermal waves. It means, namely that these waves can only develop and manifest their actual wave-features far beyond that of their own penetration length $\sigma$ in the medium. In this "cold region", such exponentially vanishing perturbations can practically not be detected experimentally. Even a "numerical detection" of their effects, e.g. in the dynamic heat-storage capacity of the slab (Section 3) requires a substantial

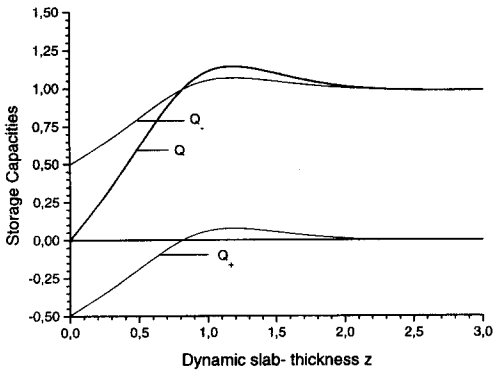


Fig. 3. The overlapping maxima at $z_1 = 1.18251$ in the total storage capacity (11) and in its components (12).

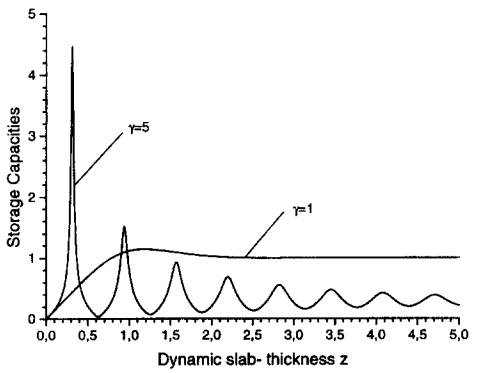


Fig. 4. Heat storage capacity of the slab for the hyperbolic heat conduction with $\gamma = 5$, compared to that of the parabolic case ($\gamma = 1$).

"numerical magnification". This is the reason why, except for the first maximum, the subsequent local minima and maxima of the storage-capacity still remained hidden. In the "hot region" $x < \sigma$, however, where the thermal effects are strong, the wave nature is still present in an "embryonic" form due to the slab-thickness less than a sixth of the wavelength. The origin of this strange situation stems from the parabolic character of Fourier's partial differential equation comprised in eqn (1). The absence of the second time-derivative in this equation (which would confer to Fourier's equation the character of a usual damped-wave-equation, similar to the "telegraphist's equation", e.g.) is equivalent to the tacit assumption of an inertialess propagation of heat with infinite signal-velocity in any medium. This implies in turn that the "wave-damping" present in Fourier's equation in the form of the first time-derivative acts necessarily on the inertialess heat transmission as an "overdamping" (similarly to the action of viscosity on the motion of a weak spring-mass system immersed in honey). The complementation of Fourier's equation to a hyperbolic form, however takes care of both, the requirement of transmission inertia as well as the finite signal velocity [3–5]. As a consequence, the wavelength is substantially reduced compared to eqn (7) and all the typical (damped) wave effects become apparent (Section 4) [6].

## 3. THE STORAGE CAPACITY

We discuss in this section the total heat-storage capacity of the slab during the half-period $\pi/\omega$ of the harmonic excitation, as well as the individual contributions of the two basic plane waves $\hat{q}_{\pm}(x, t)$ given by eqn (5), to this quantity. All these storage capacities will be considered as functions of the starting moment $t^*$ of the half-period, and the dynamic thickness of the slab, $z$.

The total loading-flux of the slab in terms of the individual contributions mentioned is:

$$\hat{q}(0, t) = [\hat{q}_+(0) + \hat{q}_-(0)]\, e^{i\omega t} = (1+i)\frac{\lambda}{\sigma} T_0\, e^{i\omega t} \tanh(1+i)z \quad (8)$$

and, thus, the heat entering the slab in a half-period across a surface of 1 m$^2$ of its boundary $x = 0$ is given by

$$Q = \frac{1}{\omega}\int_{\tau^*}^{\tau^*+\pi} Re[\hat{q}(0, t)]\, d\tau \quad (9)$$

where $\tau = \omega t$ and $\tau^* = \omega t^*$. By performing the integration we get:

$$Q = \bar{Q}(z) \cdot \cos\left[3\pi/4 + \tau^* + \arctan\left(\frac{\sin 2z}{\sinh 2z}\right)\right], \quad (10)$$

where

$$\bar{Q}(z) = \sqrt{\frac{\cosh 2z - \cos 2z}{\cosh 2z + \cos 2z}}\, Q_\infty, \quad (11)$$

and $Q_\infty = 2\sqrt{2}\lambda T_0/\omega\sigma$ represents the dynamic storage-capacity of the semi-infinite medium ($z \to \infty$) in the half-period $\pi/\omega$.

The detailed balance of the total storage-capacity in terms of individual contributions of the heat fluxes included in eqn (8) is now given by $Q = Q_+ + Q_-$ where, similarly to eqns (10)–(11):

$$Q_\pm = \mp\frac{Q_\infty}{\sqrt{2}}\sqrt{\frac{\cosh 2z \mp \sinh 2z}{\cosh 2z + \cos 2z}} \cdot \cos\left[3\pi/4 + \tau^* \mp \arctan\left(\frac{\sin 2z}{\cosh 2z \mp \sinh 2z + \cos 2z}\right)\right] \quad (12)$$

results. All the storage-capacities $Q$, and $Q_\pm$ are now functions of two independent variables, $\tau^*$ and $z$. We are interested in the (positive), maxima and minima of these functions.

By starting with $Q$, one immediately sees that this function reaches its (positive) extrema when $z = z_n$, where $z_n$ are the (positive) roots of equation

$$d\bar{Q}(z)/dz = 0, \quad \text{i.e. of } \tan 2z_n = -\tanh 2z_n \quad (13)$$

and when, at the same time, $\tau^*$ (which is obviously defined modulo $2\pi$) is chosen as:

$$\tau_n^* = \frac{5\pi}{4} - \arctan\left(\frac{\sin 2z_n}{\sinh 2z_n}\right) \tag{14}$$

The curve $-\tanh 2z$ has infinite many intersection points with the family of curves $\tan 2z$. The intersection points correspond (for $z > 0$) to the values $z = z_n$ extremizing the total heat storage capacity $Q$. For these values we also can deduce from eqn (13) a simple approximation formula:

$$z_n = (4n-1)\frac{\pi}{8}, \quad n = 1, 2, 3, \ldots \tag{15}$$

The precision of this simple approximation becomes better and better with increasing $n$. Its performance, however is already for $n = 1$ and 2 impressive. Thus compared with the values $z_1 = 1.18251$ and $z_2 = 2.7489$ obtained by numerical solving of eqn (13), eqn (15) yields $z_1 = 1.17809$ and $z_2 = 2.74889$. The iteration formula:

$$z_n^{(k)} = \frac{1}{2}[n\pi - \arctan(\tanh 2z_n^{(k-1)})], \quad k = 1, 2, 3, \ldots \tag{16}$$

improves the performance of eqn (15) again (by starting with eqn (15) as $z_1^{(0)}$, e.g., we obtain in the first and second step $z_1^{(0)} = 1.18258$ and $z_1^{(2)} = 1.18250$, respectively).

The asymptotic formula

$$\bar{Q}(z) = (1 - 2\,\mathrm{e}^{-2z}\cos 2z)Q_\infty \tag{17}$$

valid for $z \gg 1$ shows that the storage capacity of the slab does not approach the capacity $Q_\infty$ of the semi-infinite medium smoothly, but oscillates around this value indefinitely with an amplitude which decreases exponentially for increasing $z$. This is the reason why the usual computation reveals only the first, i.e. the absolute maximum, $Q_1 = 1.14299 \cdot Q_\infty$ of $Q$, corresponding to $z = z_1 = 1.18251$ and $\tau^* = \tau_1^* = 3.7949$. In order to see the subsequent local minima and maxima of $Q$, a substantial numerical magnification is necessary. The first minimum e.g., which corresponds to $z = z_2 = 2.7489$ and $\tau^* = \tau_2^* = 3.9327$, lies at $Q_2 = 0.99422 \cdot Q_\infty$, i.e. very close to the asymptotic value $Q_\infty$. In spite of these exponential weakness of the effect considered, there exists a possibility for marking the extrema of the storage capacity $\bar{Q}(z)$ graphically by making use of the "support function"

$$\tilde{Q}(z) = \frac{|\sinh 2z \cos 2z - \cosh 2z \sin 2z|}{\cosh 2z + \cos 2z} \frac{Q_\infty}{\sqrt{2}} \tag{18}$$

of $Q$ (obtained by eliminating $\tau^*$ between eqn (10) and $\partial Q/\partial \tau^* = 0$). The function eqn (18) possesses the remarkable property that its maxima are reached in the same points $z = z_n$ as the extrema of $\bar{Q}(z)$. Moreover, the two functions coincide in these and only in these points, i.e. $\tilde{Q}(z_n) = \bar{Q}(z_n)$. In other words, the total storage-capacity $\bar{Q}(z)$ which we are interested in, is such an envelope of the $\tilde{Q}(z_n)$ which lies on the maxima of this support function $\tilde{Q}(z_n)$ just with its own subsequent maxima and minima, respectively. This subtle circumstance is shown graphically in Fig. 1. The next picture, Fig. 2 shows a detail of Fig. 1, magnified around the asymptotic value $\bar{Q}/Q_\infty = 1$ so that the first maximum and minimum become visible. The $Q$-curves in Figs 1–4 are all normalized to $Q_\infty$.

With the aid of eqns (15), (7) and (6) we can express the slab-thickness $d_n$ corresponding to the extrema $\bar{Q}(z_n)$ of the total storage capacity at $z = z_n$ as follows:

$$d_n = \frac{\Lambda}{2\pi} z_n = \frac{4n-1}{16}\Lambda \tag{19}$$

Here $\Lambda$ is the wavelength of the thermal waves, and the range of validity of eqn (19) coincides, obviously with that of eqn (15). From eqn (19) results further:

$$d_{2n+1} = d_1 + n\frac{\Lambda}{2}$$

$$d_{2n+2} = d_2 + n\frac{\Lambda}{2} \tag{20}$$

Therefore, if we start with $d = d_1$ and $\tau^* = \tau_1^*$ where $Q$ reaches its absolute maximum (or with $d = d_2$ and $\tau^* = \tau_2^*$ where $Q$ reaches its first local minimum) and increase the thickness of a slab by a natural multiple of the half-wavelength $\Lambda$ and chose the starting moment $\tau^*$ according to eqn (14), the total storage capacity $Q$ jumps always from a local maximum (or minimum) to the next. This relationship between the slab-thickness and wavelength of thermal waves resembles the well known commensurability effect encountered in the case of the usual standing waves.

Let us now examine the physical relationship between the extrema of the total storage capacity $Q$ shown in Figs 1 and 2 and the slope of its components eqn (12). To this end we first calculate the partial derivative of $Q_\pm$ with respect to $z$. After some algebra we obtain that the solutions $z = z_n$ of $\partial Q_\pm(z, \tau_n^*)/\partial z = 0$ are identical with those of eqn (13). This means that for $\tau^* = \tau_n^*$ and $z = z_n$ the total storage-capacity $Q$ as well as its components $Q_\pm$ are extremized simultaneously. This circumstance may be seen in the plots of the functions eqns (11) and (12), in Fig. 3 convincingly (where eqn (12) was taken for $\tau^* = \tau_n^*$). We may thus draw the conclusion that the local maxima and minima of the total heat capacity $Q$ result from a coherent superposition of the two basic thermal waves propagating in opposite directions within the slab. The individual contributions of these two waves to the loading of the slab at $x = 0$ are obtained from (12) as:

$$Q_\pm|_{z=z_n;\tau^*=\tau_n^*} = \frac{1}{2}\left(1 \mp \frac{\sinh 2z_n}{\cosh 2z_n - \cos 2z_n}\right)\bar{Q}(z_n) \tag{21}$$

It is important to realize at this point that the direction of the energy transport due to the right-running and the left-running components of the thermal wave $\hat{q}(x, t)$, is independent of their direction of propagation which still remains unchanged in time. Indeed, as a requirement of the second law of thermodynamics (included via Fourier's law), each of the basic waves $q_{\pm}(x, t)$ transports energy across any plane $x = x_0$, $0 \leqslant x_0 \leqslant d$, of the slab from left to right when $q_{\pm}(x_0, t) > 0$ as well as from right to left when $q_{\pm}(x_0, t) < 0$, respectively, in spite of the fact that their phase velocities always point in the same direction.

In order to illustrate these results quantitatively, we have calculated the detailed balance for a slab of dynamic thickness $z_1 = 1.18251$, which corresponds (for $\tau^* = \tau_1^* = 3.7949$) to the absolute maximum $Q = Q_1 = 1.14299 \cdot Q_\infty$ of the total storage-capacity. The contribution of the components to $Q$ are $Q_+ = 0.075849 \cdot Q_\infty$, and $Q_- = 1.06714 \cdot Q_\infty$, respectively. Therefore, approximately 94% of the total storage-capacity $Q_1$ is due to the heat carried by the wave $\hat{q}_-(x, t)$ propagating from left to the right in the slab. The wave $\hat{q}_-(x, t)$ supplies an amount of 6%, only.

## 4. THE EFFECT OF HYPERBOLICITY

We close this paper by writing down the main results of the calculations carried out on the ground of the Vernotte–Cattaneo hyperbolic heat conduction equation [3, 4]:

$$\frac{\partial T}{\partial t} = a\left(\frac{\partial^2 T}{\partial x^2} - \frac{1}{c_0^2}\frac{\partial^2 T}{\partial t^2}\right) \tag{22}$$

where $c_0$ denotes the finite "signal"-velocity of the perturbations of the temperature field (for details of the following results see [6]).

In this case (indicated by a subscript $H$) the penetration length of the heat waves increases comparing to the parabolic case by the factor $\gamma$, $\sigma_H = \gamma\sigma$, while their wavelength and phase velocity decrease by the same factor, $\Lambda_H = 2\pi\sigma/\gamma$, $v_H = v/\gamma$. Comparing to $2\pi\sigma_H$ the, wavelength $\Lambda_H$ experiences even a quadratic reduction with $\gamma$, $\Lambda_H = 2\pi\sigma_H/\gamma^2$, where

$$\gamma = \sqrt{\frac{\omega a}{c_0^2} + \sqrt{1 + \left(\frac{\omega a}{c_0^2}\right)^2}} \tag{23}$$

The expression eqn (11) of the heat stored in the half period $\pi/\omega$ is substituted now by:

$$\bar{Q}_H(z) = \sqrt{\frac{2\gamma^2}{1+\gamma^4}}\sqrt{\frac{\cosh\frac{2}{\gamma}z - \cos\cos 2\gamma z}{\cosh\frac{2}{\gamma}z + \cos 2\gamma z}}\,Q_\infty \tag{24}$$

whereas the maxima and minima of $\bar{Q}(z)$ correspond in this case to the (positive) roots $z = z_n$ of equation

$$\gamma^2 \tan 2\gamma z = -\tanh\frac{2}{\gamma}z \tag{25}$$

In order to get a first insight in the effect of hyperbolicity, we have plotted this function in Fig. 4 for a finite signal velocity corresponding to $\gamma = 5$. A comparison with Fig. 1 shows dramatic differences with respect to the parabolic case. All the maxima and minima become now clearly visible. The absolute maximum is a multiple of the parabolic one and corresponds to a substantially smaller dynamic thickness of the slab. Similarly, to the parabolic case, analytic approximations allow a deeper insight into the structure of function eqn (24), again [6].

## 5. CONCLUSIONS

The main results of this paper may be summarized as follows.

1. The heat-storage capacity of a homogeneous slab excited harmonically at one and kept insulated adiabatically at the other boundary shows as a function of the slab thickness an infinite sequence of local maxima and minima which are generated by a coherent superposition of two basic thermal waves (the fundamental solutions of Fourier's equation) propagating in opposite directions along the slab. Due to the purely diffusive character of the Fourier-equation however, the subsequent extrema of the storage capacity are attenuated exponentially (the "support-curve" in Figs 1 and 2 visualizes their position). Nevertheless, in the case of thick slabs one may recognise between the slab-thickness and wavelength a commensurability relationship eqn (20) similar to that encountered in the case of the usual standing waves.
2. The main contribution to the heat stored in the slab comes from the thermal wave propagating from the excited boundary towards the adiabatic case. The other basic wave, propagating in the opposite direction, supplies to the incoming heat at $x = 0$ a contribution of about 6% only (Fig. 3).
3. For the hyperbolic heat conduction the penetration length of the heat waves increases and their wavelength decreases compared to the parabolic case. The heights and depths of the maxima and minima of the storage-capacity curve also experience a dramatic increase (Fig. 4). The practical relevance of this effect in connection with phenomena similar to that reported in [7–9] is the object of further research.

## REFERENCES

1. Balcomb, J. D., Heat storage and distribution inside passive solar buildings, LA-9694, MS.Los Alamos, New Mexico, Los Alamos Laboratory, as cited by R. W. Jones in "Analytical results for specific systems", *Passive Solar*

*Buildings*, ed. J. D. Balcomb. The MIT Press, Cambridge, MA, 1992, pp. 235–292.
2. Grigull, U. (Gröber/Erk), *Die Grundgesetze der Wärmeübertragung*. Springer-Verlag, Berlin, 1988, pp. 89–98.
3. Vernotte, P., Les paradoxes de la theorie continue de l'equation de la chleur. *Compt. Rend*, 1958, **246**(22), 3154–3155.
4. Cattaneo, C., Sur une forme de l'equation de la chaleur éliminant le paradoxe d'une propagation instantée. *Compt. Rend*, 1958, **247**(4), 431–433.
5. Tzou, D. Y., *Macro- to Microscale Heat Transfer*. Taylor and Francis, 1996.
6. Magyari, E. and Keller, B., Research Report, ETH-Zurich, 1997.
7. Tzou, D. Y., Experimental evidence for the temperature waves around a rapidly propagating crack tip. *ASME J. Heat Transfer*, 1992, **114,** 1042–1045.
8. Qiu, T. Q. and Tien, C. L., Heat transfer mechanism during short-pulse laser heating of metals. *ASME J. Heat Transfer*, 1993, **115,** 835–841.
9. Vedavarz, A., Kumar, S. and Moallemi, M. K., Significance of non-Fourier heat waves in conduction. *ASME J. Heat Transfer*, 1994, **116,** 221–224.